

Comparison of Methods for Separating Excitation Sources in Rotating Machinery

Renata Klein

R.K. Diagnostics

Gilon, D.N. Misgav, P.O. Box 101, 20103, Israel

Renata.Klein@rkdiagnostics.co.il

Abstract

Vibro-acoustic signatures are widely used for diagnostics of rotating machinery. Vibration based automatic diagnostics systems need to achieve a good separation between signals generated by different sources. The separation task may be challenging, since the effects of the different vibration sources often overlap.

In particular, there is a need to separate between natural frequencies of the structure and excitations resulting from the rotating components (signal pre-whitening), and there is a need to separate between signals generated by asynchronous components like bearings and signals generated by cyclo-stationary components like gears. Several methods were proposed to achieve the above separation tasks. The present study compares between some of these methods. For pre-whitening the study compares between liftering of the high frequencies and adaptive clutter separation. The method of adaptive clutter separation is suggested in this paper for the first time. For separating between the asynchronous and the cyclo-stationary signals the study compares between two methods: liftering in the frequency domain and dephase.

The methods are compared using both simulated signals and real data.

1 Vibration signals in rotating machinery

The diagnostic of rotating machinery via vibro-acoustic signatures requires a separation of signals excited by different rotating components. Some of the rotating components (e.g. gears) excite high vibration levels that are spread over a wide frequency band. These high vibration levels may mask other rotating components which excite lower level of vibrations. Therefore, in many cases, e.g. bearings, and especially when the diagnostic is automatic, the separation task cannot be achieved by frequency separation alone. In the case of bearings, the generated signals are relatively weak, often at high harmonics of the bearing tones. These signals may be masked by gears or blade pass frequencies.

A typical vibration signal measured on rotating machinery such as a gearbox or a jet engine is composed of several types of signals excited by the basic rotating components: gears, shafts, bearings, and rotors/blades. These signals arrive to the sensor through the structure of the machine and are therefore convolved by an impulse response function, reflecting the transmission path.

Shafts generate vibrations at several harmonics of the rotating speed with the highest amplitude at the first harmonic. The amplitudes depend on the balancing and alignment of the shaft.

Gears generate vibrations at several harmonics of the gearmesh rate with a certain amount of amplitude and frequency modulation of both gearwheel rotating speeds. The extent of modulation depends on the gear status. The frequency modulation generates a relatively large amount of sidebands that spread over a wide frequency band.

Rotor blades generate several harmonics of the blade pass frequency which is the harmonic of the shaft speed corresponding to the number of blades on the rotor.

Bearings with localized faults generate shocks for every contact occurrence with the deteriorated surface. The shocks excite resonances of the structure between the bearing and the sensor. The shock amplitude is modulated when the fault is on a rotating surface that is subject to variations of load and/or changes of the transmission path to the sensor. When assuming no slippage, the rate of shock occurrences (kinematic frequencies) can be calculated from the bearing geometry. The kinematic frequencies are non-integer multiples of the rotating speed of the shaft. Due to slippage, the shock rate may change randomly with about

1-2% tolerances around the kinematic rates. Therefore the signals generated by a faulty bearing are asynchronous to the rotating speed.

The signals generated by shafts, gears and blades will be manifested in the spectrum at discrete frequencies which are integer multiples of the corresponding shaft speed, i.e. synchronous to the rotating speed. All these signals are strong compared to the signals generated by defective bearings.

The measured signal is thus composed of a superposition of signals corresponding to the rotating components multiplied in the frequency domain by a structural transfer function.

2 Separation of discrete frequency noise

In bearing diagnostics, one of the first tasks is to separate the bearing signals from the discrete frequency noise [1], [2], [3], i.e. signals generated by shafts, gears, rotors, etc. Several methods were proposed for this task [2]: linear prediction, dephase (removal of the time synchronous average) [1], [3], discrete/random separation, and liftering in the quefrequency domain. The goal is to remove the synchronous elements of the vibration signal, leaving the asynchronous vibrations, which are usually related to the structure and the bearings.

In this study two methods for separation of discrete frequency noise are compared, dephase and filtering in the quefrequency domain [2]. These two methods enable removal of specific peaks synchronous to specific shafts.

2.1 Dephase

The method is based on removal of the phase averaged signal (or the synchronous time average – STA) [1], [3]. The synchronous time average is the mean value of segments representing one rotation of a shaft. The STA removes the asynchronous components by averaging the resampled signal over a cycle of rotation. All the signal elements that are not in phase with the rotating speed are eliminated, leaving the periodic elements represented in one cycle, i.e. the elements corresponding to harmonics of the shaft rotating speed.

In the cycle domain the STA y_n corresponding to rotation frequency R_1 of the cycle history x is calculated as follows:

$$y_n := \frac{1}{M} \sum_{m=0}^{M-1} x_{n+mN} \quad n = 1, \dots, N \quad (1)$$

where $N = 1/R_1$ and M is the number of cycles in the signal. Note that y is a vector in \mathbb{R}^N representing a single cycle.

The phase average y is replicated in order to get a vector of the same size as x (the resampled signal):

$$z_n = y_{n \bmod N} \quad n \in \mathbb{N} \quad (2)$$

Now removing the phase average, thereby generating the dephased signal, removes all the effects which are synchronous with the rotating speed R_1 .

$$\tilde{x} = x - z \quad (3)$$

The basic dephase algorithm removes the STA of the entire signal and is therefore appropriate for stationary signals. Its performance depends on the accuracy of the measurement and the accuracy of the rotating speed analysis.

The adapted dephase [6] removes the STA in running frames. It is able to remove the STA from non-stationary signals where the amplitudes of the synchronous elements may change (due to varying rotating speeds and loads). The recommended frame size depends on the amount of variations in operating conditions such as load and rotating speed.

In some cases, where several asynchronous shafts exist, the procedure needs to be repeated for each shaft rotating speed separately. Removing the STA of shaft R_1 from the signal resampled by R_2 is a little trickier, since the R_2 -resampled signal is not periodic with any period associated with R_1 .

Instead of taking the raw data, R_1 dephased signal is resampled by R_2 . This signal already had the R_1 effects removed from it. After resampling the signal, the elements that are synchronous with R_2 can be

removed. This process is repeated with all shafts. Finally the signal is resampled back to the desired cycle domain (R_k).

When K STAs corresponding to synchronous shafts $R_k, k = 1, \dots, K$ (e.g. shafts of a gearbox) need to be removed, the procedure can be simplified as follows:

- The raw signal is resampled only once according to one of the shafts rotating speed R_1 . It is recommended to start with the fastest shaft.
- The STA corresponding to R_1 is removed (dephase by R_1)
- For all $k - 1$ remaining shafts:
 - The dephased signal is interpolated to another shaft $R_k, k = 2, \dots, K$ with a sampling rate proportional to the actual sampling rate. If the resampling was done for the fastest rotating shaft, a linear interpolation will be sufficient.
 - The STA corresponding to R_k is removed.
- The dephased signal is reversed to the desired cycle or time domain using interpolation.

When applying the simplified procedure, the algorithm computation load is significantly reduced. This is because the most demanding task in the sequence is resampling, which usually applies both linear interpolation and spline interpolation.

The spectrum of a dephased signal is expected to reveal peaks related to the asynchronous tones of deteriorated bearings and to the structural natural frequencies.

2.2 Liftering in the quefreny domain

The most general definition of cepstrum $C(\tau)$ (complex cepstrum) [2], [5] is:

$$C(\tau) = \mathcal{F}^{-1}[\log(X(f))]; \forall X(f) = \mathcal{F}[x(t)] = A(f)e^{j\varphi(t)} \quad (4)$$

when

$$\log[X(f)] = \log[A(f)] + j\varphi(t) \quad (5)$$

and when $x(t)$ is the the time or cycle history and $X(f)$ is the respective Fourier transform (in the frequency or order domain) .

The power or real cepstrum is defined as the inverse Fourier transform of the log power spectrum.

$$C(\tau) = \mathcal{F}^{-1}[\log(|X(f)|)] = A(f) \quad (6)$$

The difference between the real and the complex cepstrum is that the complex cepstrum contains the phase information from the spectrum allowing reconstruction of the signal in the time domain while the real cepstrum allows only reconstruction of the power spectrum. The drawback of the complex cepstrum is that the phase should be unwrapped before the inverse Fourier transform. This is not feasible for a random signal with discontinuous phase and therefore not applicable for vibration signals of rotating machinery.

The abscissa of the cepstrum, τ , has units of time but it is called quefreny. All the terminology related to cepstrum is a result of syllables interchange in the regular terms: harmonics become rhamonics, filtering is called liftering, etc.

A relatively new method to reconstruct the signals while using the real cepstrum was proposed by R.B. Randall and J. Antoni [5]. The idea is to keep the phase of the Fourier transform, then to calculate the real cepstrum and when reversing from the frequency domain to the time domain to reuse the phase of the Fourier transform (see Figure 1). This method allows usage of cepstrum for separation of different parts of the spectrum in vibration of rotating machinery. It takes advantage of the fact that, because the Fourier transform of the logarithm, the multiplication in the frequency domain become addition in the quefreny domain and it permits the liftering of such terms. The liftering can be performed using any type of window.

The cepstrum combines families of sidebands or any multiple peaks with similar distances in the spectrum into several rhamonics of peaks in the quefreny domain. Therefore by removing the rhamonics from the cepstrum, these families of peaks are removed from the spectrum. The cepstrum can be calculated based on the frequency spectrum or based on the order spectrum (the spectrum of the signal after phase resampling). The signal that is reconstructed after removing all the families of sidebands in the order spectrum, i.e. removing the modulation of the tooth gearmesh, contains only the asynchronous parts of the original signal (mainly bearings and transmission path effects).

The efficiency of liftering the rhamonics corresponding to a family of equidistant peaks in the spectrum depends on the frequency/order resolution of the spectrum. Therefore it is preferable to use large frames, i.e. long periods of time. Liftering is most effective when the peaks in the spectrum are sharp and of high amplitude. Variations of the rotating speed may smear the peaks, affecting the ability to remove the discrete frequencies. Therefore it is recommended to use the order domain spectrum where the peaks are sharp.

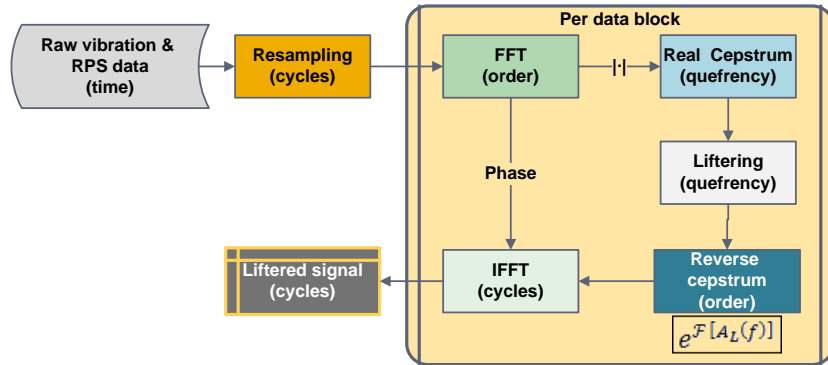


Figure 1: Flow chart of quefrequency liftering

3 Transmission path estimation

After removal of the discrete frequency "noise", the weak bearing signal may be still masked in some frequency bands due to the transmission path effect that may attenuate some frequency bands and/or amplify others. Division of the spectrum after removal of the discrete frequencies by the transfer function is expected to whiten the spectrum. The whitened signal will contain mainly the bearing excitations.

In order to estimate the transfer function of the transmission path, all peaks corresponding to the rotating components should be removed, i.e. the discrete frequencies related to shafts, gears, and blades as well as the bearing tones.

The determination of the transmission path transfer function is valuable also for detection of structural changes, or for "whitening" the signals of other components. The transfer function should be evaluated in the frequency domain when the goal is to detect structural changes and in the order domain when the focus is on bearing diagnostic.

There are several algorithms that can be used to estimate the transmission path transfer function [2]: minimum entropy deconvolution, liftering of the high quefrequencies [5] and a new algorithm that performs an adaptive clutter separation of the spectrum.

The study compares two methods, i.e. liftering of high quefrequencies and adaptive clutter separation. Both methods allow the prewhitening of the signal for bearing tones enhancement and the estimation of the transmission path effect.

3.1 Liftering of high quefrequencies

The liftering of high quefrequencies [5] is taking advantage of the reconstruction of the signal after editing the real cepstrum and reversing to the time domain using the phase of the Fourier transform (the procedure was described in 2.2). Since estimation of transmission path requires removal of all the sharp peaks in the spectrum, this will correspond to liftering all high quefrequencies, i.e. windowing the cepstrum at low quefrequencies.

When the signal is stationary with a relatively constant rotating speed this can be done by calculating the cepstrum based on the frequency spectrum. When analyzing a transient with varying rotating speed it would be required to calculate the cepstrum based on the order spectrum and then, after reconstruction of the signal, to resample it back to the time domain.

3.2 Adaptive clutter separation

The algorithm for adaptive clutter separation (ACS) is described in Figure 2. In essence, the algorithm separates between the sharp peaks in a spectrum and the "background noise". It was designed for peaks removal from spectra but it can be used for any signal. The algorithm estimates the smoothed "background noise" of a spectrum by calculating a configurable percentile of spectrum values in overlapping dynamic

blocks. It is assumed that the smoothed "background noise" represents the transmission path effects and the peaks are related to rotating components. The algorithm is expected to be most effective when the spectrum contains numerous sharp peaks that can be differentiated from the background. The block size increases in proportion to the rotating speed variations or can be kept constant. The change in the block size was designed to avoid influence of smeared peaks at high frequencies on the evaluated transmission.

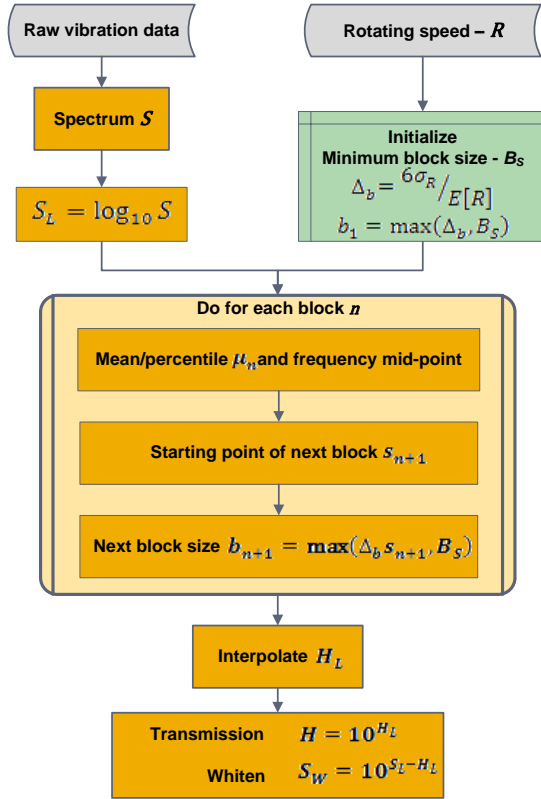


Figure 2: Flowchart of the ACS algorithm

The adaptive clutter separation algorithm can be applied in frequency or in order spectra. In the frequency domain it is usually applied with a dynamic block size and in the order domain with a constant block size.

The whiten signal can be constructed by applying the procedure described in Figure 3. This procedure was inspired by the method for reconstruction of signals which was proposed in [5].

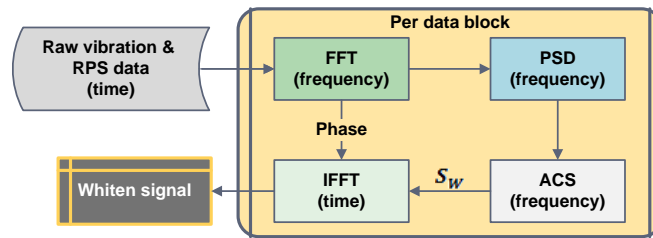


Figure 3: Signal whitening with ACS algorithm

4 Data analysis procedure

The methods were compared using two sets of data: a dataset of simulated signals and an actual data dataset measured in a gearbox (PHM'09 challenge labeled data set). The simulated dataset was selected because it allows full control of the data elements. In this study the evaluation of the ability to isolate the transmission path effects is achievable only with the simulated dataset. The PHM'09 dataset was selected because it contains data measured on a gearbox with a large number of faults in the gears and bearings that challenge the separation capabilities of the evaluated methods.

4.1 The simulated dataset

The following model is used to simulate the vibrations signal. Let R_1, \dots, R_K be the rotating speeds of the simulated shafts and denote by Φ_1, \dots, Φ_K the respective phase functions. For each shaft k let $p_{k,1}, \dots, p_{k,M_k}$ be the relative frequencies (orders) of the parts which are mounted on shaft k . Denote by $\theta_{k,1}, \dots, \theta_{k,M_k}$ the phase shifts of these rotating parts. The phase of each rotating part can be described by $\alpha_{k,i}(t) = p_{k,i}\Phi_k(t) + \theta_{k,i}$. Then the signal is described by:

$$x(t) = \sum_{k=1}^K \sum_{i=1}^{M_k} A_{k,i} \cos \alpha_{k,i}(t) + n(t) \quad (7)$$

where $n(t)$ is white noise and $A_{k,i}$ is the amplitude of a rotating part signal.

In a real machine, the rotating parts excitations $X(\omega)$ give rise to responses at the sensor through the machinery's structure transfer function $H(\omega)$ which amplifies each frequency range differently $Y(\omega) = X(\omega)H(\omega)$. The resulting signal is:

$$y(t) = x(t) * h(t) = \left[\sum_{k=1}^K \sum_{i=1}^{M_k} A_{k,i} \cos \alpha_{k,i}(t) + n(t) \right] * h(t) \quad (8)$$

The vibration signal was composed using two sets of rotating speeds (R_1 and R_2) corresponding to asynchronous shafts. The signal included components synchronous with rotating speed R_1 with different amplitudes at harmonics 1, 2, 3, 19, 38, 57. It also included components synchronous with rotating speed R_2 with different amplitudes at harmonics 1, 2, 3, 17, 32, 34, 51, 64, 96. In addition gear like components with gear meshes at order 61 and 183 of R_2 and 83 of R_1 with FM (frequency modulation) by the respective rotating speed were added.

All the amplitudes of the synchronous elements ($A_{k,i}$ for $k = 1, 2$ corresponding to R_1 and R_2) were constant. The added white noise SNR was 10 dB. Shaft R_1 and R_2 rotating speeds were on average 20Hz and 40Hz respectively with added white noise of $\sigma \sim 0.02Hz$. Similar signals were simulated four times, i.e. two records of the same situation and two sensors (named s3 and s5). In each record of sensor s5 asynchronous elements simulating different bearing faults have been added (see specification of the bearing tones and respective amplitude modulation in Table 1).

Record	Bearing tone	Side bands [order]		Natural freq. [Hz]	
1	BSF	5.29	R2	0.03	10,392
2	BSF1	5.29	R2	0.13	10,392
3	BSF2	5.29	R2	0.548	10,392
4	Comb1	7.21	none		4,503
		5.29	R2	0.03	10,392
		5.29	R1	0.03	11,432
5	Comb2	7.21	none		4,503
		8.82	R2	1	5,543
6	IR1	8.82	R2	1	5,543
7	IR2	3.00	R2	1	5,543
8	IR3	3.00	R2	1	5,543

Table 1: Specifications of bearing signals in the simulation data set

All the simulated signals were convolved with an impulse response obtained from a Finite Elements model of a bearing house. Each record was simulated in two files of 10 seconds sampled at 40 kHz – the data set contains a total of 16 raw data files.

4.2 Analysis of the simulated dataset

The data set of simulated signals was used to compare both the separation of discrete frequency noise as well as the transmission path effect.

Figure 4 shows the block diagram describing the analysis process. The left branch was designed to compare the performance of the algorithms for estimation of the transmission path effect. The right branch was designed for comparison of the algorithms for discrete frequencies separation. The comparison between the two algorithms for discrete frequencies separation was carried out on the signal dephased in respect to R_1 . Several blocks have been added to the right branch for comparison of the algorithms for transmission path estimation in the order domain, i.e. lifter high quefrecencies and ACS.

The spectra in the frequency domain were calculated with a resolution of 0.3 Hz. The data was resampled according to R_1 with 4096 samples per cycle and with 2048 samples per R_2 cycle. All the spectra in order domain were calculated with a resolution of 0.015 order.

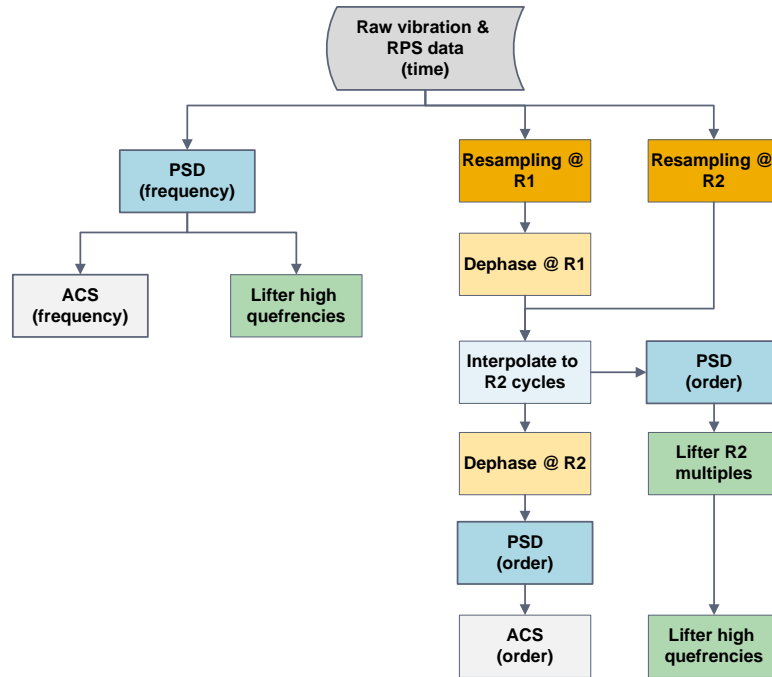


Figure 4: Block diagram of the analysis of the simulation dataset

4.3 PHM'09 Challenge data

The PHM'09 data set included 280 recordings of 4 seconds each, measured on the gearbox described in Figure 5, using two vibration sensors (Sin and Sout) and a tachometer. All the bearings were similar. Some of the signals were recorded when the gearbox was in 'spur' configuration, and others when it was in 'helical' configuration. Data were collected at 30, 35, 40, 45 and 50 Hz shaft speeds, under high and low loading (HL and LL).

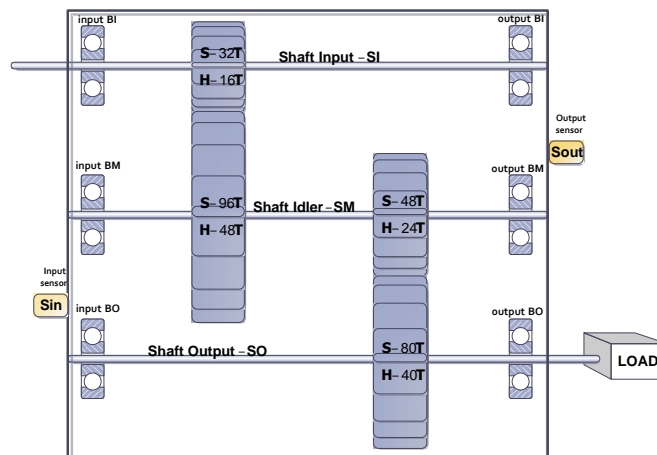


Figure 5: Challenge apparatus: spur (S) and helical (H) configurations (from [4])

In the challenge apparatus, in spur and helical configurations, the idler shaft (SM) and the output shaft (SO) rotated at 1/3 and 1/5 of the rotating speed of the input shaft (SI) correspondingly. The gear ratios generated overlapping characteristic frequencies.

Table 2 summarizes the recordings of the PHM'09 data set and the damages that were present.

Case	Gears				Bearings			Shaft	
	32T	96T	48T	80T	bSI	bSM	bSO	Input	Output
Spur 1	Good	Good	Good	Good	Good	Good	Good	Good	Good
Spur 2	Chipped	Good	Eccentric	Good	Good	Good	Good	Good	Good
Spur 3	Good	Good	Eccentric	Good	Good	Good	Good	Good	Good
Spur 4	Good	Good	Eccentric	Broken	Ball	Good	Good	Good	Good
Spur 5	Chipped	Good	Eccentric	Broken	Inner	Ball	Outer	Imbalance	Good
Spur 6	Good	Good	Good	Broken	Inner	Ball	Outer	Imbalance	Good
Spur 7	Good	Good	Good	Good	Inner	Good	Good	Good	Key
Spur 8	Good	Good	Good	Good	Inner	Ball	Outer	Imbalance	Good
	16T	48T	24T	40T					
Helical 1	Good	Good	Chipped	Good	Good	Good	Good	Good	Good
Helical 2	Good	Good	Broken	Good	Comb	Inner	Good	Bent	Good
Helical 3	Good	Good	Good	Good	Comb	Ball	Good	Imbalance	Good
Helical 4	Good	Good	Good	Good	Comb	Ball	Good	Imbalance	Good
Helical 5	Good	Good	Broken	Good	Inner	Good	Good	Imbalance	Good
Helical 6	Good	Good	Good	Good	Inner	Good	Good	Bent Shaft	Good

Table 2: PHM'09 challenge dataset faults

4.4 Analysis of the PHM'09 challenge data

The data from the PHM'09 challenge was used only to compare methods for the separation of discrete frequencies since the transmission path effect was not known.

Figure 6 shows the block diagram describing the analysis process. Due to the fact that the idler and output shaft rotated at exact multiples of the input shaft rotating speed it was not required to remove separately the synchronous average of the input shaft. The block diagram in Figure 6 illustrates the dephase method that applied resampling only once, followed by interpolation from cycles corresponding to one shaft to another (see detailed explanation in 2.1).

The data was resampled according to SI with 4096 samples per cycle. All the spectra in order domain were calculated with a resolution of 0.015 order.

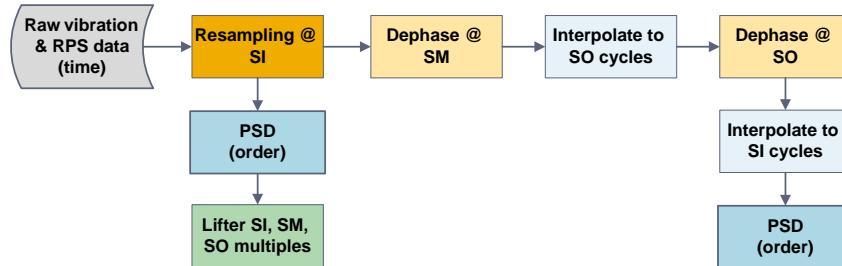


Figure 6: Block diagram of the analysis of the PHM'09 challenge dataset

5 Results

5.1 Discrete frequencies separation

The comparison was performed using both the simulated dataset and the PHM'09 challenge records. The performance measure, p_r , was defined as the percentage of removed RMS, at the harmonics of the respective shafts orders (9).

$$p_r = 100 \left[1 - \sqrt{\frac{\sum_{i \in A} P_{A,i} \cdot \Delta o}{\sum_{i \in A} P_i \cdot \Delta o}} \right] \quad (9)$$

where P is the original order spectrum in G^2/order , P_A is the spectrum obtained after application of the algorithm in G^2/order , Δo is the order spectrum resolution, and A is a set of indices corresponding to the removed rotating speed harmonics (of all shafts). p_r was computed by both methods, dephase and quefrequency liftering, for each data record.

The percentage of removed RMS obtained by both methods in the simulated dataset and in the PHM'09 challenge recordings are presented in Figure 10 and in Figure 11 respectively. In the simulated dataset and in most of the PHM'09 records the percentage removed by dephase is above 80%. In the simulated dataset the method of quefrequency liftering is below 80% and in PHM'09 records it is below 60%. The percentage removed by dephase is always higher than the percentage removed by liftering in the quefrequency domain.

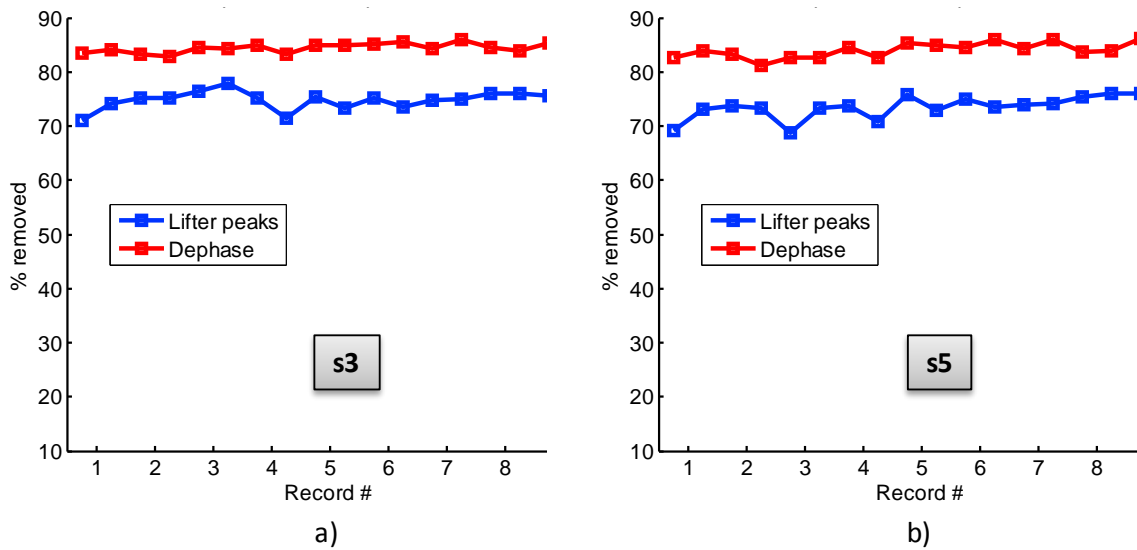


Figure 7: Percentage of RMS removed, simulated dataset: a) sensor s3, b) sensor s5

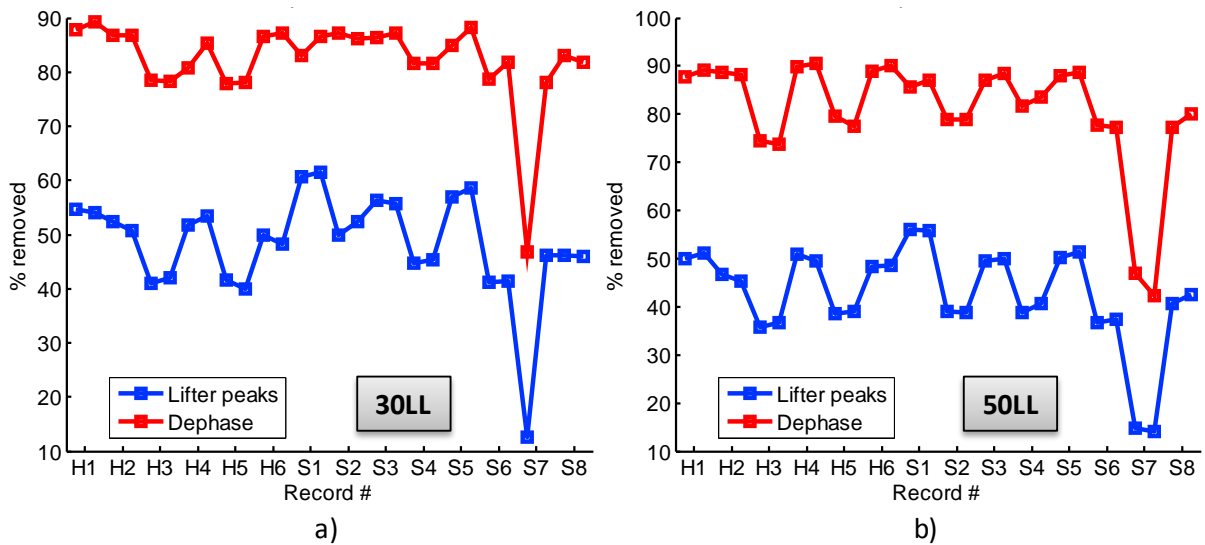


Figure 8: Percentage of RMS removed, PHM'09 challenge dataset, sensor Sin: a) records with rotating speed of 30Hz low load, b) records with rotating speed of 50Hz low load

Figure 9 presents an example of the results in the order spectrum for both datasets. In this graphs it can be observed that all the peaks related to the gears where reduced by dephase to the level of the "background noise" while the level reduction of the liftering in the quefrequency domain was significantly lower.

Moreover, in Figure 9b, it can be observed that several peaks that belong to bearings remain clearly in the dephased spectrum despite their proximity to the gear sidebands which were completely removed (reduction by approximately a decade). At the same situation, the quefrequency liftering succeeded to remove the gear sidebands only partially.

The results show that the dephase method is superior relative to the method of liftering in the quefrequency domain.

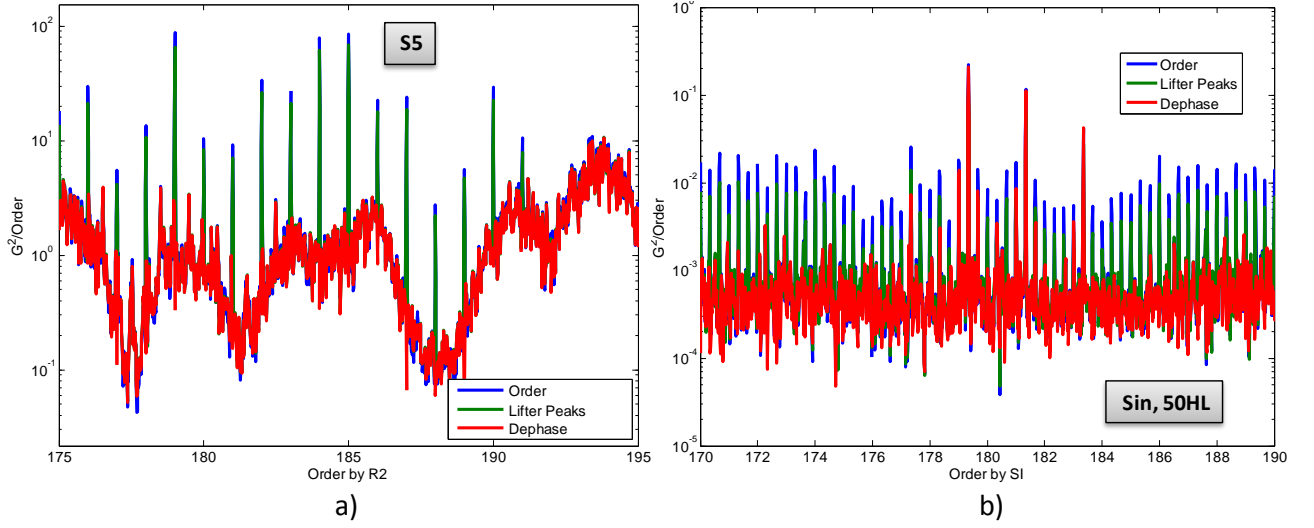


Figure 9: Sections of order spectra, original spectrum – blue, liftered spectrum – green, dephase – red: a) simulated data set, order by R_2 , sensor s5, b) PHM dataset, order by SI, sensor Sin, 50Hz, high load

5.2 Transmission path effects

The transfer function was estimated using both methods of adaptive clutter separation and liftering of the high quefrequencies, for the simulated dataset, in the frequency and in the order domain. For analysis purposes, we have overlaid and visually inspected four types of graphs: the spectra of the original signal, the simulated transfer function, the transfer function that was estimated using adaptive clutter separation, and the transfer function obtained by liftering the high quefrequencies (Figure 12). In addition, and in order to quantify the comparison results, the mean distance d_r between the transfer function estimations and the actual simulated transfer function was calculated (10). Let $T(f)$ be the actual transfer function, f denoting either frequency or order (in our case order according to R_2) and $T_A(f)$ be the transfer function estimated with one of the algorithms, the mean distance d_r in dB is:

$$d_r = \frac{20}{N} \sum_{i=1}^N |\log_{10} T_A(f_i) - \log_{10} T(f_i)| \quad (10)$$

The mean distance represents the estimation error of the respective algorithms. The results in the order and frequency spectra are presented in Figure 10 and Figure 11 respectively.

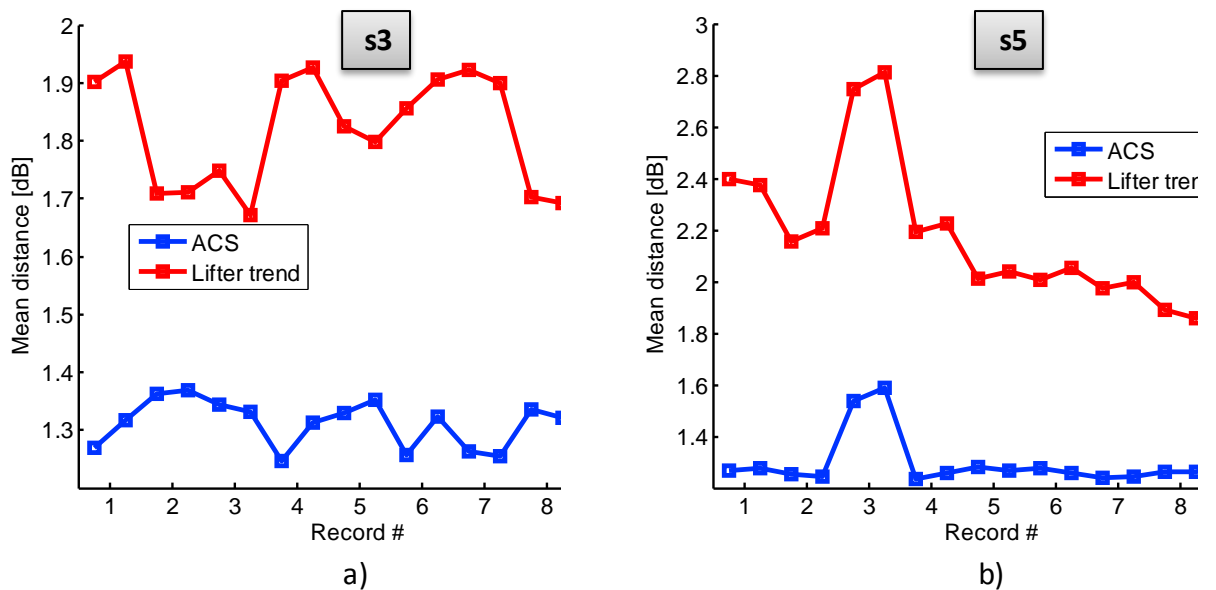


Figure 10: Mean distance in the order by R_2 domain of the simulated dataset: a) sensor s3, b) sensor s5

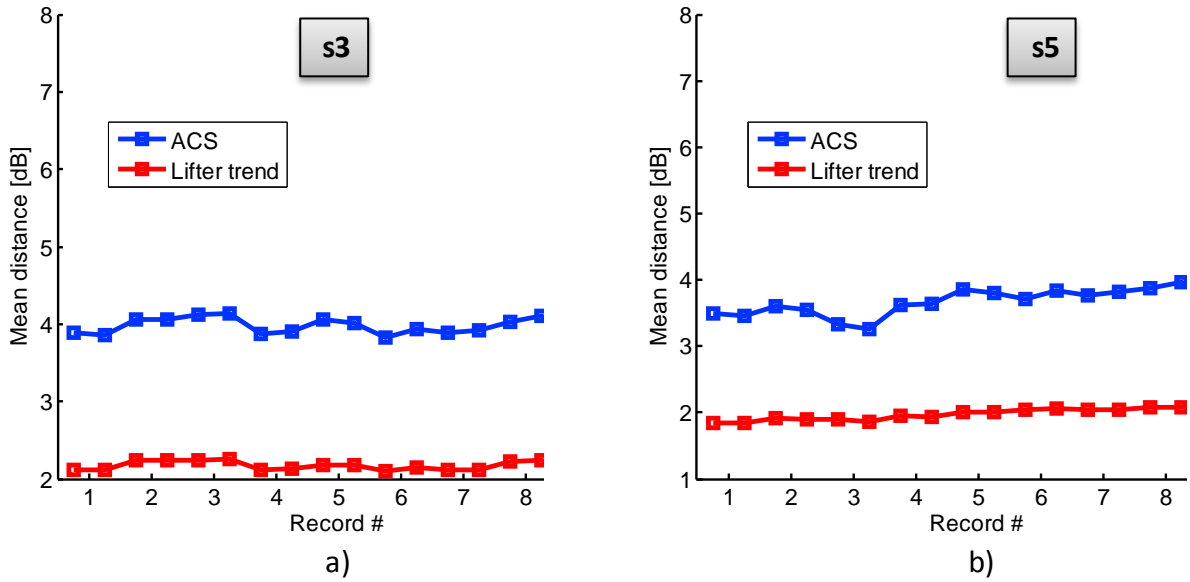


Figure 11: Mean distance in the frequency domain of the simulated dataset: a) sensor s3, b) sensor s5

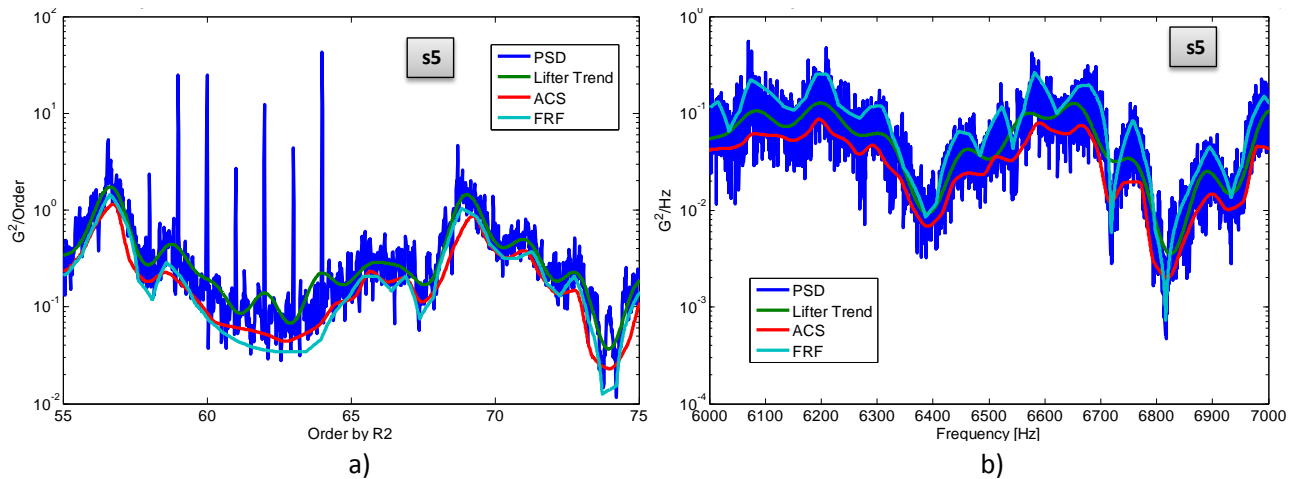


Figure 12: Sections of PSDs of s5 in the simulated dataset. Original PSD – blue, Liftered spectrum – green, ACS – red, Simulated transfer function – cyan. a) Order spectrum by R_2 , b) Frequency spectrum

In the order domain (Figure 10), the ACS mean distance from the actual transfer function is lower than 1.6 dB and always lower compared to the liftering distance. For sensor s5 (Figure 10b) the mean distance of liftering is ~ 2.4 dB and the mean distance of ACS is ~ 1.4 dB. The performance difference is more emphasized for sensor s5, which contains the additional impulses of the bearings. The difference between s3 and s5 is explained by the capability of ACS to discriminate between background and peaks. Therefore it can be concluded that ACS was found superior to liftering in the order domain.

On the other hand, in the frequency domain (Figure 11) the liftering method was found superior to ACS. In Figure 11 the distances from the actual transfer function for each method are almost constant for the different simulated records with an approximate constant difference between ACS and liftering (2 dB for s3 and 1.5 dB for s5). We attribute the poorer performance of ACS in the frequency domain to the fact that it was designed to separate between relatively sharp peaks and the "background noise". When the spectrum does not have prominent peaks over the background the algorithm performance is less satisfactory. Figure 12 illustrates the big difference between the spectra in frequency and order domains; in the frequency domain the peaks are smeared and cannot be distinguished while in the order domain the peaks are sharp. The other important observation that can be made by inspecting Figure 12 is the fact that both algorithms of ACS and liftering are able to estimate and correctly track the actual transfer function.

In summary, for finding the transfer function in the frequency domain, the liftering of the high frequencies is recommended. For whitening the signal for diagnosis of rotating components in the order

domain, the ACS method provides better results. For this purpose, ACS can be applied in the order domain, and then the signal can be reconstructed in the cycles domain and interpolated back to the time domain.

6 Conclusions

The paper compared between two methods for separation of discrete frequencies noise and between two methods for isolation of transmission path effects.

For separation of discrete frequencies noise, the method of dephase was found superior relative to quefrequency liftering. In the case of synchronous shaft speeds, a modified flow of algorithms was suggested for efficient realization of the dephase process.

A new method for isolation of transmission path effects, adaptive clutter separation (ACS), was proposed. The method was compared to cepstrum liftering. In the frequency domain, cepstrum liftering was found superior to ACS. In the order domain, ACS provided better results. It seems that ACS is more effective for prewhitening while cepstrum liftering is preferable for estimation of transmission path effects.

References

- [1] N. Sawalhi, R.B. Randall, *Localised fault diagnosis in rolling element bearings in gearboxes*, Proceedings of The Fifth International Conference on Condition Monitoring and Machinery Failure Prevention Technologies – CM/MFPT 2008.
- [2] R.B. Randall, J. Antoni, *Rolling element bearing diagnostics – A tutorial*, Mechanical Systems and Signal Processing 25 (2011), pp. 485-520.
- [3] R. Klein, E. Rudyk, E. Masad, M. Issacharoff, *Emphasizing Bearing Tones for Prognostics*, The International Journal of Condition Monitoring, Vol. 1, (2011), Issue 2, pp. 73-78.
- [4] R. Klein, E. Rudyk, E. Masad, M. Issacharoff, *Model Based Approach for Identification of Gears and Bearings Failure Modes*, International Journal of Prognostics and Health Management, ISSN 2153-2648, 2011 008.
- [5] R.B. Randall, B. Peeters, J. Antoni, S. Manzato, *New cepstral methods of signal pre-processing for operational modal analysis*, Proceedings of ISMA2012-USD2012, Leuven, Belgium, 2012, pp. 755-764.
- [6] R. Klein, E. Rudyk, E. Masad, *Bearing diagnostics in non-stationary environment*, International Journal of Condition Monitoring, March 2012.